Femtosecond laser capsulotomy

Neil J. Friedman, MD, Daniel V. Palanker, PhD, Georg Schuele, PhD, Dan Andersen, MS,
George Marcellino, PhD, Barry S. Seibel, MD, Juan Batlle, MD, Rafael Feliz, MD,
Jonathan H. Talamo, MD, Mark S. Blumenkranz, MD, William W. Culbertson, MD

PURPOSE: To evaluate a femtosecond laser system to create the capsulotomy.

SETTING: Porcine and cadaver eye studies were performed at OptiMedica Corp., Santa Clara, California, USA; the human trial was performed at the Centro Laser, Santo Domingo, Dominican Republic.

DESIGN: Experimental and clinical study.

METHODS: Capsulotomies performed by an optical coherence tomography–guided femtosecond laser were evaluated in porcine and human cadaver eyes. Subsequently, the procedure was performed in 39 patients as part of a prospective randomized study of femtosecond laser-assisted cataract surgery. The accuracy of the capsulotomy size, shape, and centration were quantified and capsulotomy strength was assessed in the porcine eyes.

RESULTS: Laser-created capsulotomies were significantly more precise in size and shape than manually created capsulorhexes. In the patient eyes, the deviation from the intended diameter of the resected capsule disk was 29 μm ± 26 (SD) for the laser technique and 337 ± 258 μm for the manual technique. The mean deviation from circularity was 6% and 20%, respectively. The center of the laser capsulotomies was within 77 ± 47 μm of the intended position. All capsulotomies were complete, with no radial nicks or tears. The strength of laser capsulotomies (porcine subgroup) decreased with increasing pulse energy: 152 ± 21 mN for 3 μJ, 121 ± 16 mN for 6 μJ, and 113 ± 23 mN for 10 μJ. The strength of the manual capsulorhexes was 65 ± 21 mN.

CONCLUSION: The femtosecond laser produced capsulotomies that were more precise, accurate, reproducible, and stronger than those created with the conventional manual technique.

Financial Disclosure: The authors have equity interest in OptiMedica Corp., which manufactures the femtosecond laser cataract system.

J Cataract Refract Surg 2011; 37:1189–1198 © 2011 ASCRS and ESCRS

Cataract surgery is the most common operation in the United States; more than 3 million patients have the procedure every year.[1,2] Despite the significant improvements in surgical technique over the past 4 decades, the critical steps are still manual procedures. The most important and difficult maneuver to master, creating the continuous circular capsulorhexis,[3,4] is performed by freehand tearing of the capsule with a cystotome and/or a capsule forceps relying on visual clues (ie, the pupillary margin) and is therefore highly dependent on surgical skills and complicating factors. Even in the most experienced hands, an optimal capsulorhexis is not always achieved. The procedure is especially challenging in cases of borderline pupillary dilation, shallow anterior chambers, weak zonules, poor visibility, pediatric cataracts, mature cataracts, and fibrosed capsules.

A properly constructed capsulorhexis improves the safety of hydrodissection, nuclear disassembly and removal, and cortical cleanup and inhibits posterior capsule opacification.[4–13] The ideal capsulorhexis is a well-centered circular opening slightly smaller than the intraocular lens (IOL) optic so the anterior capsule completely covers the edge of the optic by 0.5 mm for 360 degrees. This ensures that the IOL is contained in the capsular bag close to the effective lens position (ELP), which is assumed in IOL calculation formulas; thus, the refractive outcome of the surgery will be as precise and predictable as possible. The performance of newer IOLs, including multifocal, aspheric, and accommodating designs ("premium" IOLs), is more sensitive to accurate positioning and would benefit from more reproducible sizing, shaping, and centration of the anterior capsulotomy.[14] Furthermore,

misalignment of the IOL, especially a multifocal IOL, which is more likely with a suboptimally constructed capsulorhexis, produces bothersome or even disabling optical aberrations. Although experienced surgeons usually achieve excellent and consistent outcomes, increased precision in sizing, shaping, and centration of the capsulotomy, as well as reproducibility and safety, would improve results, particularly for premium IOLs.

Femtosecond lasers are able to create exquisitely precise, customizable incisions in ocular tissue without collateral damage, and the safety of this approach has been demonstrated in millions of corneal procedures over the past 10 years. In cataract surgery, all the corneal (wound, side port, relaxing) and lenticular (capsulotomy, segmentation, fragmentation) incisions can be performed by the laser prior to entering the globe with the surgical instruments. However, unlike corneal flaps for refractive surgery, cataract incisions are placed deep inside the eye and their precise alignment on target tissues should be based on a 3-dimensional (3-D) map of the patient's eye. We report a novel anterior capsulotomy technique with an optical coherence tomography (OCT)-guided femtosecond pattern-scanning laser (Catalys Precision Laser System, OptiMedica Corp.) that significantly increases the precision and reproducibility of cataract surgery. The integrated OCT maps the anterior segment of the eye 3 dimensionally to ensure exact placement of the cutting pattern. The anterior capsulotomies produced with this technique were stronger and more precise than manually created capsulorhexes. Although lens segmentation and corneal incisions were

Corresponding author: Neil J. Friedman, MD, Mid-Peninsula Ophthalmology Medical Group, 900 Welch Road, Suite 402, Palo Alto, California 94304, USA. E-mail: njfmd@pol.net.

also performed, this article focuses on the capsulotomy results.

MATERIALS AND METHODS

Laser System

The laser system has been described in detail[15] and can be summarized briefly. It consists of a 3-D scanning femtosecond laser (1.03 μm wavelength, 400 femtosecond pulse duration, up to 10 μJ pulse energy, 12 to 80 kHz repetition rate, and 10 μm focal spot size) that is optically combined with long-range spectral-domain OCT (<11 μm depth resolution, >12 mm image depth), as well as near-infrared video imaging. The system allows localization and imaging of the corneal and lens surfaces with the OCT and creates a 3-D automatic treatment plan for the laser based on these data. The laser scanner then precisely places the selected patterns in the target structures. Typical spot spacing for the laser ranged from 5 to 20 μm laterally and 10 to 30 μm in depth, depending on the desired effect to be achieved.

Ex Vivo Porcine and Human Cadaver Eyes

The quality of femtosecond laser cutting in the lens capsule was evaluated in freshly enucleated porcine eyes. The crystalline lens was removed from the eye, placed horizontally with the anterior surface facing up in a container filled with balanced salt solution (BSS, Alcon Labs), and covered with a thin (#1) cover slip. A spiral laser pattern was applied vertically from above through the cover slip starting 200 μm under the anterior capsule and ending 200 μm above the capsule. The threshold energy and optimized pattern spot density to produce a continuous cut were determined by lasering approximately 100 porcine lens samples (Figure 1). These parameters were used for the subsequent laser procedures.[15]

A specialized instrument to evaluate the strength of the cut capsule edge in porcine eyes was built. It consisted of 2 semicircular pins with a 2.0 mm radius of curvature attached to motorized translation stages to stretch the tissue at a constant rate and piezoelectric dynamometers on both sides to
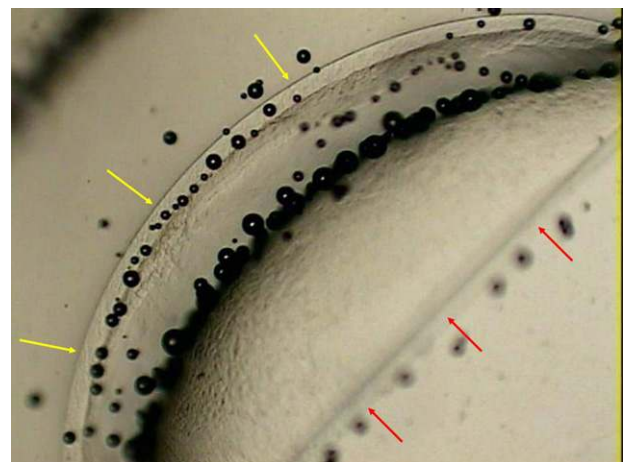

Figure 1. Femtosecond laser capsulotomy of a porcine lens capsule demonstrating the sharp edges of the cut capsule (*yellow arrows*) and the opposite edge, which rolled out of the microscope focus after dissection (*red arrows*).
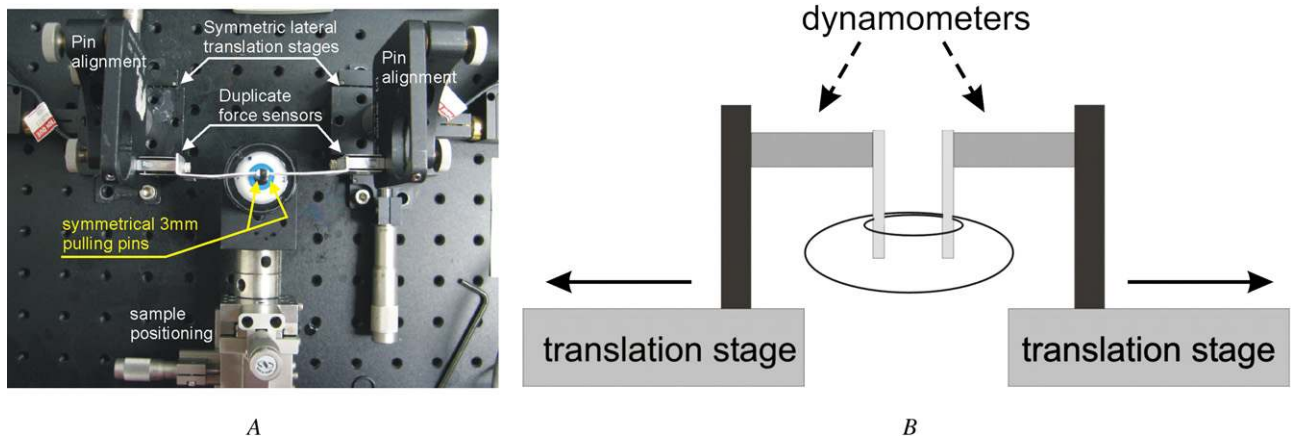
Figure 2. Photograph (*A*) and simplified diagram (*B*) of the capsule stretching apparatus.

register and record the applied force. One of 2 procedures was used: a 4.6 mm laser capsulotomy performed with pulse energies of 3 to 10 µJ, 5 µm lateral spot spacing, and 10 µm depth spacing or a 5.0 mm manual capsulorhexis performed in situ by an experienced cataract surgeon (N.J.F.). The eyes were prepared by removing the cornea and iris, stabilizing the open globe on a metal holder, and placing the globe in a bath with BSS to optically bridge the gap between the contact lens and the sample. Once the capsule opening was created, the lens was removed with phacoemulsification using a Legacy 20 000 machine (Alcon Laboratories, Inc.) and the capsular bag was filled with a low-viscosity liquid containing 0.05% gelatin. The pins were then inserted into the capsulotomy opening and pulled symmetrically in opposite directions at 0.25 mm/second until the capsule ruptured (Figure 2).

For scanning electron microscopy (SEM) imaging, additional testing was performed in approximately 100 enucleated human eyes. Instead of removing the lens from the eye, only the cornea and iris were removed to better preserve the lens and allow lasing of the lens in an otherwise whole globe. These samples were also submerged in a container with BSS and covered with a thin cover slip. The scanning laser parameters for creating a capsulotomy in the human lens samples were similar to those used in the porcine samples.

In Vivo Human Study

All surgery was performed at the Centro Laser, Santo Domingo, Dominican Republic, after institutional review board approval of the study protocol for laser-assisted cataract surgery was obtained from the Dominican Republic Independent Review Board (Conabios, Santo Domingo) and informed consent was obtained from all participants. Laser-assisted cataract surgery was performed in 1 eye of the patients; the fellow eye served as a control for manual cataract surgery in some of the patients.

Patients were eligible for the study if they had grade 1 to 4 nuclear sclerotic cataracts according to the Lens Opacities Classification System III (LOCS III),[16] understood the informed consent document, and were able to comply with the treatment and follow-up schedule. Additional inclusion criteria were Early Treatment of Diabetic Retinopathy Study corrected distance visual acuity worse than 20/30, pupillary dilation of at least 7.0 mm, and axial length between 22.0 mm

and 26.0 mm. Exclusion criteria included enrollment in another drug or device study within the prior 3 months, history of ocular trauma, or coexisting ocular disease affecting vision or ocular surgery (except previous cataract surgery in the fellow eye), anterior chamber depth less than 2.5 mm, or corneal astigmatism greater than 5 diopters (D). The patients were 55 to 80 years of age (70 years ± 6 [SD]), 60% were women and 40% men. The full range of nuclear sclerotic lens grades (1 to 4) was represented, with more than 50% of patients having LOCS grade 3 or 4 cataract.

Treatment eyes were dilated with 1 drop each of cyclopentolate 1.0% and phenylephrine 2.5% (3 doses at 20-minute intervals) and scopolamine 0.25% (2 doses at 20-minute intervals) starting 1 hour before the laser procedure. One drop of flurbiprofen 0.03% was also administered 40 minutes before surgery, and a Honan balloon was applied to the eye
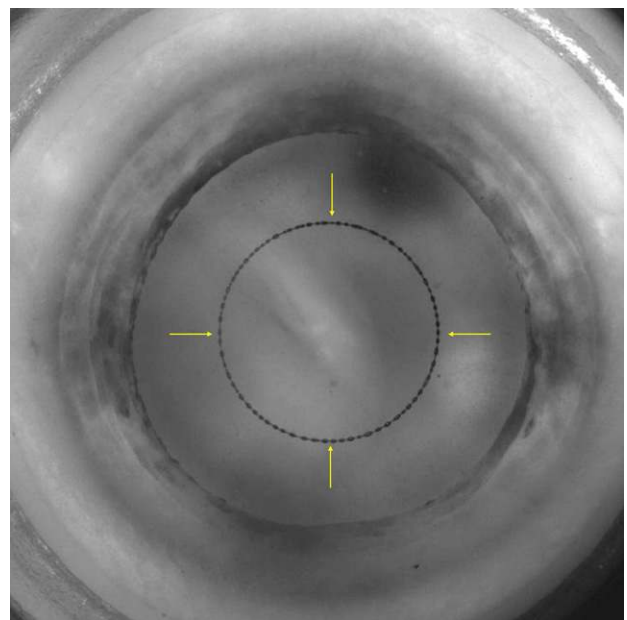

Figure 3. Infrared video camera image of the complete laser capsulotomy demonstrating the bubbles filling the circular line of the laser cut.
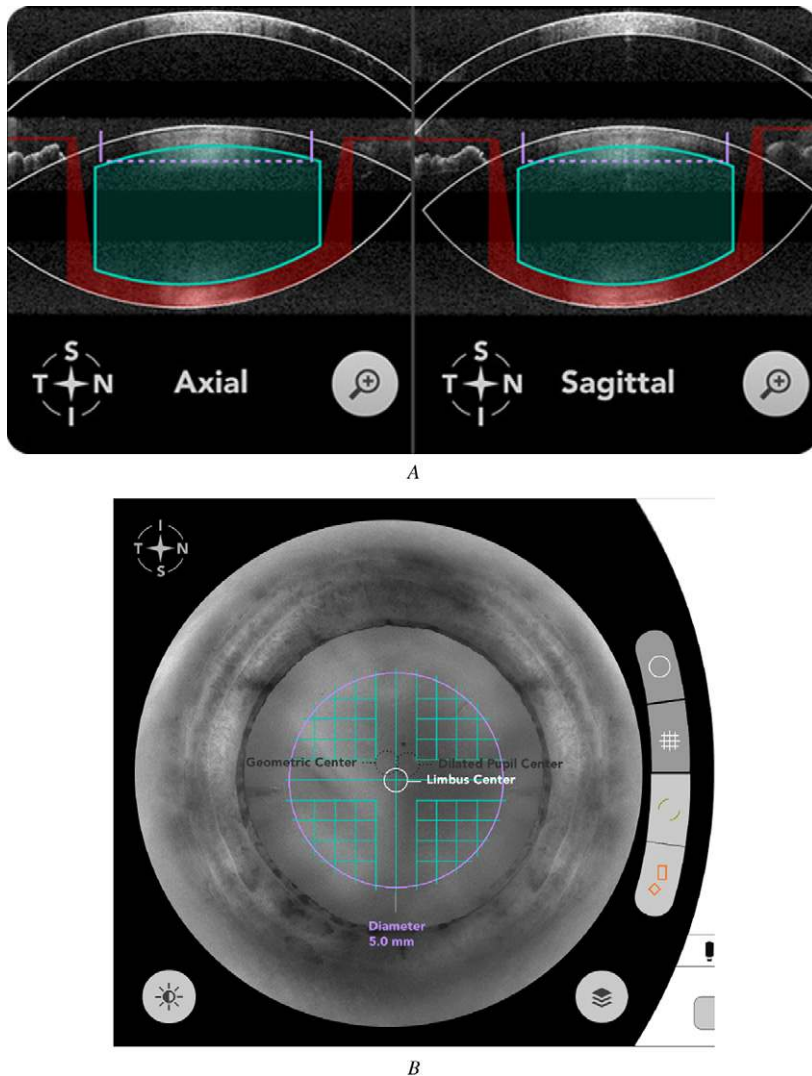
A

B

Figure 4. Screen shots of the femtosecond pattern-scanning laser showing OCT and system near-infrared video. *A*: The OCT image of the eye with outlined boundaries of the cornea and lens capsule. The capsulotomy pattern and lens fragmentation pattern are shown in solid purple and green, respectively. *B*: View of the eye via the near-infrared video camera, with overlaid guidance lines indicating a planned capsulotomy pattern (*purple*) and lens fragmentation pattern (*green*).

for the final 10 to 15 minutes. Following administration of a topical anesthetic agent (1 drop of proparacaine hydrochloride 0.5%), the patient's eye was docked to the system using a suction device coupled to the laser. After the anterior segment structures were imaged, processed, and displayed with the integrated OCT, the surgeon selected the treatment patterns and, if necessary, adjusted the laser parameters based on the anatomy and orientation of the eye. After that, a 4.6 mm diameter capsulotomy was performed (Figure 3). All patients were then treated with lens fragmentation patterns; some were also treated with corneal incisions delivered precisely to the intended tissue location.

Stable positioning during laser treatment was achieved by the LiquidOptics patient interface (OptiMedica Corp.), consisting of a suction ring and liquid immersion lens. This approach enables docking to occur with only a small rise in the intraocular pressure (15 mm Hg), avoiding patient discomfort or amaurosis. In addition, the cornea does not fold because no hard lens surface contacts the patient's cornea directly. Avoiding corneal folds is very important for precise cutting as folds distort the beam.

Once the laser system is coupled to the eye through docking, a long-range spectral-domain OCT imaging system is used to obtain a 3-D map of the patient's anterior segment and both surfaces of the lens, and the near-infrared video provides a live image of the eye. Image processing software automatically identifies anterior and posterior corneal surfaces, iris, and anterior and posterior lens surfaces (Figure 4, *A*) and overlays the prospective capsulotomy and lens fragmentation patterns on the OCT data on a graphic user interface for the surgeon's review. The overlaid near-infrared video enables the surgeon to verify lateral position of the laser patterns and control every aspect of the laser cuts (Figure 4, *B*). The capsulotomy pattern is a posterior to anterior spiral, starting in the anterior lens tissue and terminating in the lower end of the anterior chamber to ensure intersection of the incision with the anterior lens capsule in between. The upward direction of laser energy propagation prevents scattering of the laser beam prior to its focal point on microbubbles that form in the previously treated locations. Instead, the bubbles, which are located below the current laser focus, scatter the laser beam propagating beyond the focal spot and decrease the amount of laser radiation reaching adjacent structures, especially blocking light from reaching the retina. The laser capsulotomy was completed in approximately 2.5 seconds, with laser parameters

Table 1. Capsule rupture force after manual capsulorhexis and laser capsulotomy with different pulse energies.

Parameter	Manual	Laser		
		3 µJ	6 µJ	10 µJ
Mean capsule rupture force (mN)	65 ± 21	152 ± 21	121 ± 16	113 ± 23
Number of samples	13	11	13	9

determined in the preclinical experiments (eg, 3 µJ, 5 µm lateral spot spacing, and 20 µm depth spacing).

After the laser treatments were executed, the patients were transferred to a sterile operating room and phacoemulsification and implantation of a foldable IOL with a 6.0 mm optic (Alcon Acrysof IQ SN60WF) were performed. The excised capsule disk was extracted with a forceps and saved for measurements with light microscopy.

The resected anterior capsule disks were prepared for digital light microscopy by rinsing them in saline, staining them with 0.5% trypan blue, and placing them between glass slides. For histology, the disks were fixed in 1% paraformaldehyde and embedded in paraffin. For SEM, the samples were fixed in 2.5% glutaraldehyde in sodium cacodylate buffer, post-fixed in 1% osmium tetroxide, dehydrated in a series of methanols, critical point dried, and plasma coated with gold palladium.

Measurements of Capsulotomy Size and Centration

Following staining, the size and shape of the capsule disk samples were measured with digital light microscopy using a National Institute of Standards and Technology traceable reference standard. Size was measured by placing the greatest linear dimension of each sample along the x-axis and calculating a mean of 4 measurements: the width along the horizontal, vertical, and 2 oblique meridians (at 45 degrees). Circularity of the sample was measured as a normalized ratio of the sample area to the area of a disk, with the diameter corresponding to the maximum width of the sample. (This ratio is 1 for an ideal circle.)

During surgery, immediately after its removal, the capsule disk was flattened on the cornea and its diameter measured with calipers; an intraocular cross-sectional measurement of the capsulotomy opening was then taken with a Seibel rhexis ruler (MicroSurgical Technology). One week and 1 month after surgery, a dilated eye examination was
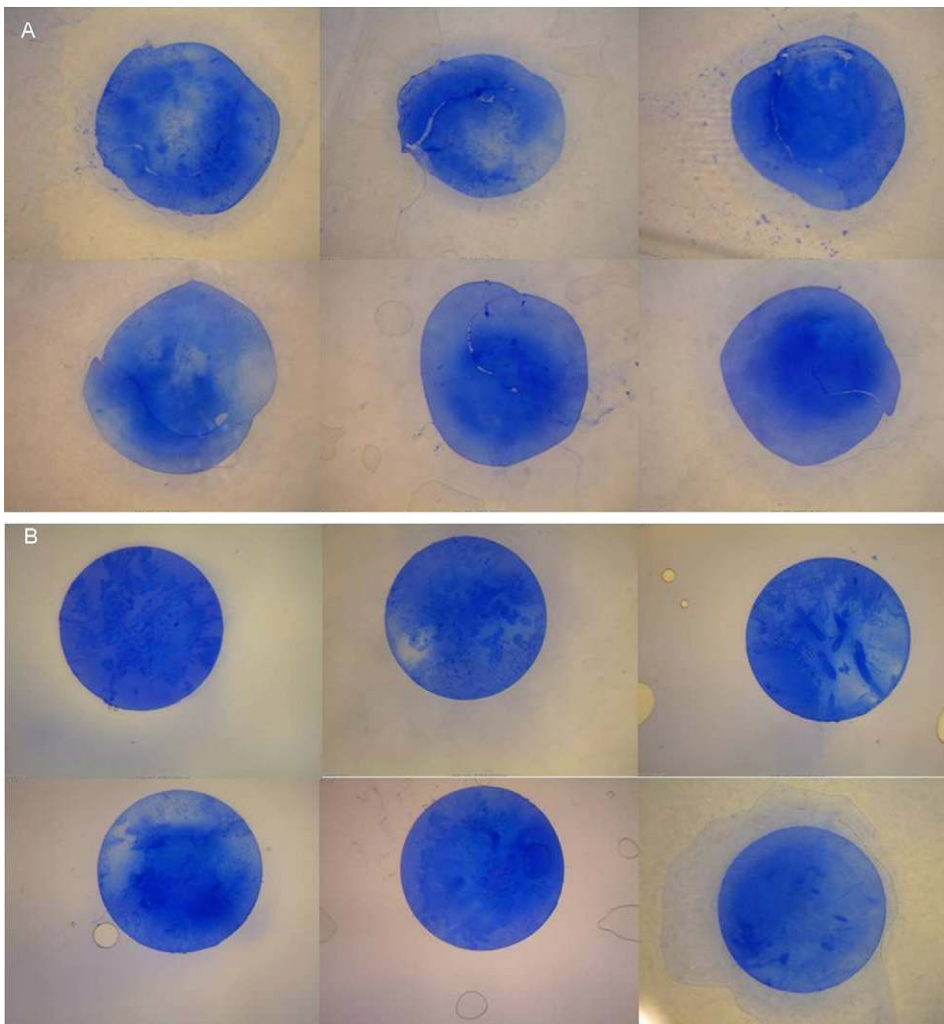

Figure 5. Excised and stained lens capsule samples from a manual capsulorhexis (*A*) and a laser capsulotomy (*B*).

Table 2. Capsulotomy size and shape of the extracted lens capsules.

Procedure	Target Diameter (mm)	Deviation from Intended (μm)*	Sample Size	Circularity*	Circularity Sample Size
Manual capsulorhexis	5.0	337 ± 258	23	0.80 ± 0.15	18
Laser capsulotomy	4.6	29 ± 26	39	0.94 ± 0.04	39

*Mean ± SD

done and anterior segment digital photographs were obtained with a slitlamp. The size and centration of the capsulotomy were subsequently calculated based on the digital images. The images were scaled by comparing them with the known size of the IOL optic.

RESULTS

Ex Vivo Porcine Eyes

Forty-six porcine eyes were studied; 13 had a manual capsulorhexis and 33, a laser capsulotomy. The strength of the capsule after manual capsulorhexis and after laser capsulotomy was assessed with the previously described capsule-stretching instrument. The mean strength of the capsule after manual capsulorhexis and laser capsulotomy is shown in Table 1. The differences were statistically significant ($P < .05$) and suggest that a laser-created capsulotomy may be more than twice as strong as a capsulorhexis created manually.

In Vivo Human Study

Thirty-nine patients were included. Laser-assisted cataract surgery was performed in 1 eye of all patients; the fellow eye of 24 patients served as a control for manual cataract surgery. All patients tolerated the surgery well. The laser capsulotomy cuts were complete, with no radial nicks or tears, and no complications attributable to the laser treatments occurred. Samples of the extracted capsules are shown in Figure 5. The size and circularity of the extracted capsule disks were measured as described earlier, and the values are summarized in Table 2. In some manual capsulorhexis cases, only parts of the excised capsules could be retrieved and analyzed, which reduced the number of cases for some measurements. The difference between the mean deviation from the intended size of the manual capsulorhexes and the laser capsulotomies was statistically significant ($P < .05$). Similarly, the difference between the mean shape (circularity ratio) of the manual capsulorhexes and the laser capsulotomies was statistically significant ($P < .05$).

Figure 6 and Table 3 summarize the variation in the capsule opening over time for both techniques. At each time point, the absolute difference and deviation from the intended capsule opening diameter was smaller in

the laser capsulotomy group than in the manual capsulorhexis group. With both techniques, the opening enlarged during surgery by about 400 μm when the extracted disk was compared with the opening measured right after disk removal. After removal of the crystalline lens and implantation of the IOL, the size of the anterior capsule opening returned to a value close to its intended dimension.

The position of the laser capsulotomies was within 77 ± 47 μm of the intended centration within the dilated pupil (Figure 7). The typical appearances of the manual capsulorhexis and laser capsulotomy in a slitlamp examination the day after surgery are shown in Figure 8. The images illustrate more precise central position and proper sizing of the laser capsule opening, resulting in a complete and symmetric 0.7 mm overlap
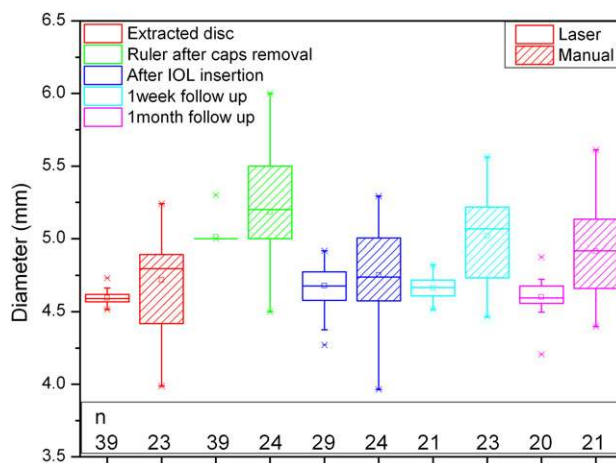

Figure 6. Boxplots of the capsule sizing for laser capsulotomy and manual CCC at different time points of the cataract procedure and follow up: extracted disk = diameter of the extracted capsule disk, as in Table 2; ruler after caps removal = diameter measured with Seibel rhexis ruler immediately after capsule disk removal; after IOL insertion = diameter measured after implantation and last manipulation of the IOL, analyzed from surgical video, with IOL as sizing reference; 1-week follow-up = diameter measured from an anterior chamber slitlamp image taken at the 1-week follow-up visit, with IOL as sizing reference; 1-month follow-up = diameter measured from anterior chamber slitlamp image taken at the 1-month follow-up visit, with IOL as sizing reference. The box is determined by the central mean as well as the 25th and 75th percentiles. The whiskers are determined by the 5th and 95th percentiles.

Table 3. Capsule opening diameter after manual and laser cutting at various postoperative times.

Technique	Extracted Disk	Capsule Opening Diameter (mm)			
		After Caps Removal	After IOL Insertion	At 1 Week	At 1 Month
Manual capsulorhexis diameter (mm)	4.66 ± 0.26	5.18 ± 0.42	4.75 ± 0.31	5.02 ± 0.30	4.92 ± 0.34
Laser capsulotomy diameter (mm)	4.57 ± 0.03	5.01 ± 0.06	4.68 ± 0.16	4.66 ± 0.07	4.60 ± 0.13

All results are mean ± SD.

of the capsular bag on the edge of the 6.0 mm IOL optic. The smooth and continuous capsule edge is also apparent. Scanning electron microscopy images of the capsule edge produced by manual capsulorhexis and laser capsulotomy are shown in Figure 9. Note the laser-induced microgrooves (arrows in Figure 9, B) with dimensions far below the resolution of an ophthalmic microscope.

DISCUSSION

An integrated OCT-guided femtosecond laser system enabled precise cutting of the anterior lens capsule. The system created continuous sharp-edged anterior capsulotomies of exact size, shape, and position. Compared with the manual capsulorhexis technique, the laser method improved precision in sizing the capsulotomy by 12 times and accuracy in shaping the capsulotomy by a factor of approximately 3. The tensile strength of the resulting capsule opening was greater than that of the manual capsulorhexis by a factor of more than 2; this property could decrease the risk for inadvertent rupture during subsequent steps of cataract surgery.

Similar improvement in capsule edge strength has been reported with another laser system.[A] The weaker edge in the manual capsulorhexis could be because tissue that is stretched to the limit of breakage is likely to be weakened in the areas adjacent to the line of rupture. Another reason could be that manual capsulorhexis results in a less uniform shape, having areas with a smaller radius of curvature, which creates higher stress during stretching. The porcine capsule is thicker and more difficult to tear than the human capsule. It reacts like a pediatric human capsule (ie, more elastic) and is stretched to create a manual capsulorhexis tear, which is different from the tissue response in an adult human eye. The capsule strength was measured in porcine eyes only, so the results may not be applicable to human eyes.

The accuracy and predictability of the laser capsulotomy size was better at all time points. The transient enlargement noted during surgery probably results from the stretching and retraction of the lens capsule after the capsule opening is created and resolves after the crystalline lens has been removed from the bag.

Femtosecond technology has the ability to facilitate and optimize manual portions of cataract surgery.[15,17,18] The benefits are increased safety and improved refractive outcomes. A symmetric, well-centered, and appropriately sized anterior capsulotomy is essential for maximizing IOL performance, and this is even more critical for premium IOLs (ie, toric, multifocal, and accommodating IOLs). The ability to produce a perfect capsulotomy for any IOL design is extremely valuable since capsulotomy construction directly influences the ELP,[14,19] which is a major source of error in IOL power calculations.[20]

The actual axial position of the IOL is significantly influenced by the configuration of the capsulorhexis. Complete overlap of the optic secures the IOL in the capsular bag, raising the likelihood that the IOL will reside in its predicted position. A capsulorhexis that is too large or asymmetric will not overlap or will only partially overlap the IOL optic, allowing postoperative contractile forces of the capsule to shift the IOL
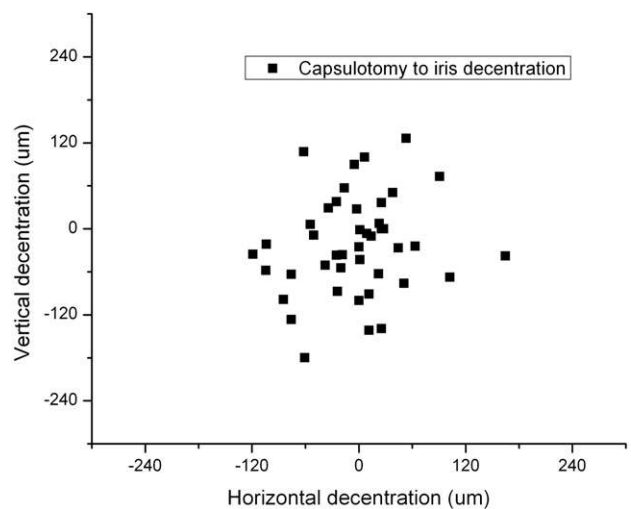

Figure 7. Centration of laser capsulotomy relative to center of the dilated pupil taken from the system near-infrared video after laser capsulotomy.
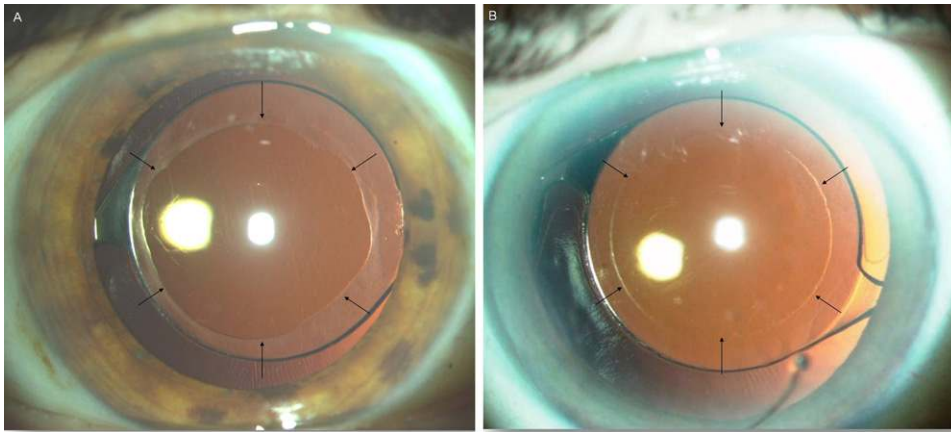
Figure 8. Slitlamp view of the edge of the capsule on the day after surgery for manual capsulorhexis (*A*) and laser capsulotomy (*B*).

anterior to its predicted location or cause tilt, inducing a myopic shift or astigmatism, respectively. A capsulorhexis that is too small can result in posterior IOL movement with a hyperopic shift as well as capsule phimosis that can interfere with vision. In most human eyes, a 0.5 mm change in IOL position results in approximately 1.0 D change in refractive error; however, this figure increases for higher-power IOLs and decreases for lower-power IOLs and can vary from less than 0.5 D to 1.5 D or more in some situations.[21,22] The tolerance for position error for toric and multifocal IOLs is even less, so small amounts of tilt, decentration, or rotation of these IOLs can result in significant deviations from the desired refractive outcome as well as symptomatic visual aberrations.[23,24] A poorly constructed capsulorhexis may even preclude implantation of certain IOL designs. Therefore, a method of reproducibly creating a precisely sized and centered anterior capsulotomy should improve the predictability of refractive outcomes.

Current IOLs are designed to center in the capsular bag, but this does not always occur. When performing the capsulorhexis, surgeons attempt to center the opening by using the pupillary margin as a reference point; therefore, we chose to align the capsulotomies in this study by positioning them on the pupil center. However, other positions (ie, geometric center of the lens or center of the visual axis) may be advantageous. In addition, a custom-shaped or decentered capsule opening may be useful for future IOL designs and for stabilizing an IOL in a purposely off-center position (ie, with optic capture or asymmetric haptics), such as for treating strabismus.[25] The laser-guiding software and integrated OCT image processing allow the surgeon to choose the capsulotomy centration method and alter the capsulotomy position immediately prior to applying the laser pulses. This degree of customization and precision is unattainable with a manual technique.

Various conditions can make successful creation of a manual capsulorhexis difficult, including poor capsule visibility, borderline pupillary dilation, shallow anterior chambers, weak zonules, fibrotic capsules, absence of the red reflex, intumescent mature cataracts, or elastic (pediatric) capsules. Methods to facilitate creating the capsulorhexis by tracing or drawing the desired opening have been developed.[26–28] However, all have limitations: Circular imprints on the cornea and intraocular rulers are only rough guides; mechanical devices can weaken or tear the capsule; using a high-frequency electrosurgical probe can cause

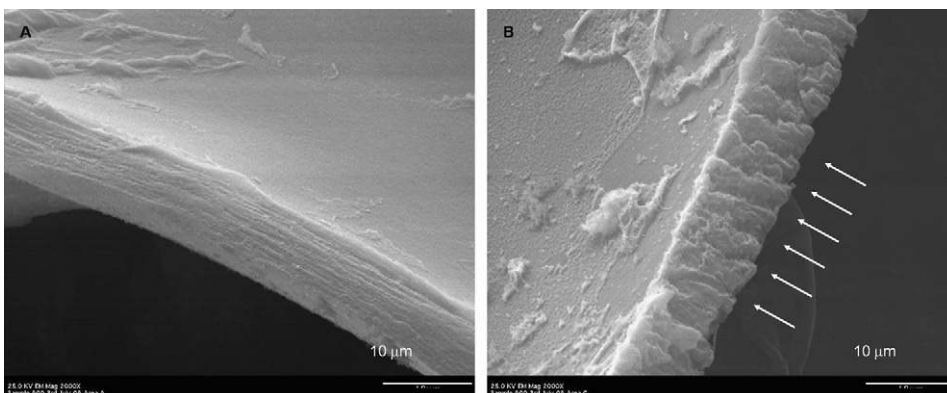

Figure 9. Scanning electron micrographs of the excised capsule disk edge produced by manual capsulorhexis (*A*) and laser capsulotomy (*B*). White arrows in *B* point to the microgrooves produced by the laser pulses (bar = 10 μm).

thermal damage and weaken biomechanical stability of the capsule[26,27,29]; using a vitrector can cause radial tears in up to 7.7% of cases[30]; and using the Fugo blade (a bipolar continuous radiofrequency cutter) can increase the risk for radial tears.[28,30,31] Another electrosurgical device, the pulsed-electron avalanche knife, can produce a capsulotomy without thermal damage or radial tears.[32–34] Nevertheless, these are still manual procedures and as such, accompanied by the inherent difficulties of producing an accurately centered, sized, and shaped capsulotomy.

An essential aspect of the femtosecond laser system used in this study that differentiates it from femtosecond lasers designed to create laser in situ keratomileusis flaps is the integrated OCT that performs 3-D mapping of the cornea and lens. The system automatically aligns all incision patterns in 3-D to follow the contour of ocular structures, which minimizes the degree of required cutting overlap and optimizes the safety zone distances. This critical feature guarantees safe, precise, and reproducible placement of the cutting patterns within the target tissue.

In conclusion, the OCT-integrated femtosecond laser system allows exact placement of cutting patterns in ocular tissue and can therefore achieve a level of precision unattainable with manual and mechanical techniques. The femtosecond laser optimizes the anterior capsulotomy by creating a continuous sharp-edged capsule cut with increased strength. The system has multiple benefits for cataract surgery.

REFERENCES

1. Harmon D, Thomas D. 2010 Annual Survey of US Cataract Surgeons. Market Scope June 2010. Abstract available at: http://dev.market-scope.com/market_reports/2009/06/2007-annual-cataract-surgeon-s.html. Accessed April 23, 2011
2. Cullen KA, Hall MJ, Golosinskiy A. Ambulatory surgery in the United States, 2006. Natl Health Stat Report 2009; 28:1–25. Available at: http://www.cdc.gov/nchs/data/nhsr/nhsr011.pdf. Accessed April 23, 2011
3. Dooley IJ, O'Brien PD. Subjective difficulty of each stage of phacoemulsification cataract surgery performed by basic surgical trainees. J Cataract Refract Surg 2006; 32:604–608
4. Gimbel HV, Neuhann T. Development, advantages, and methods of the continuous circular capsulorhexis technique. J Cataract Refract Surg 1990; 16:31–37
5. Neuhann T. Theorie und Operationstechnik der Kapsulorhexis [Theory and surgical technic of capsulorhexis]. Klin Monatsbl Augenheilkd 1987; 190:542–545
6. Assia EI, Apple DJ, Tsai JC, Lim ES. The elastic properties of the lens capsule in capsulorhexis. Am J Ophthalmol 1991; 111:628–632
7. Krag S, Thim K, Corydon L. Strength of the lens capsule during hydroexpression of the nucleus. J Cataract Refract Surg 1993; 19:205–208
8. Peng Q, Apple DJ, Visessook N, Werner L, Pandey SK, Escobar-Gomez M, Schoderbek R, Guindi A. Surgical prevention of posterior capsule opacification. Part 2: enhancement of cortical cleanup by focusing on hydrodissection. J Cataract Refract Surg 2000; 26:188–197
9. Wasserman D, Apple DJ, Castaneda VE, Tsai JC, Morgan RC, Assia EI. Anterior capsular tears and loop fixation of posterior chamber intraocular lenses. Ophthalmology 1991; 98:425–431
10. Ram J, Apple DJ, Peng Q, Visessook N, Auffarth GU, Schoderbek RJ Jr, Ready EL. Update on fixation of rigid and foldable posterior chamber intraocular lenses. Part I. Elimination of fixation-induced decentration to achieve precise optical correction and visual rehabilitation. Ophthalmology 1999; 106:883–890
11. Hollick EJ, Spalton DJ, Meacock WR. The effect of capsulorhexis size on posterior capsular opacification: one-year results of a randomized prospective trial. Am J Ophthalmol 1999; 128:271–279
12. Assia EI, Apple DJ, Tsai JC, Morgan RC. Mechanism of radial tear formation and extension after anterior capsulectomy. Ophthalmology 1991; 98:432–437
13. Aasuri MK, Kompella VB, Majji AB. Risk factors for and management of dropped nucleus during phacoemulsification. J Cataract Refract Surg 2001; 27:1428–1432
14. Çekiç O, Batman C. The relationship between capsulorhexis size and anterior chamber depth relation. Ophthalmic Surg Lasers 1999; 30:185–190; correction, 714
15. Palanker DV, Blumenkranz MS, Andersen D, Wiltberger M, Marcellino G, Gooding P, Angeley D, Schuele G, Woodley B, Simoneau M, Friedman NJ, Seibel B, Batlle J, Feliz R, Talamo J, Culbertson W. Femtosecond laser-assisted cataract surgery with integrated optical coherence tomography. Sci Transl Med 2010; 2:; 58ra85
16. Chylack LT Jr, Wolfe JK, Singer DM, Leske MC, Bullimore MA, Bailey IL, Friend J, McCarthy D, Wu S-Y; Longitudinal Study of Cataract Study Group. The Lens Opacities Classification System III. Arch Ophthalmol 1993; 111:831–836. Available at: http://archopht.ama-assn.org/cgi/reprint/111/6/831. Accessed April 23, 2011
17. Nagy Z, Takacs A, Filkorn T, Sarayba M. Initial clinical evaluation of an intraocular femtosecond laser in cataract surgery. J Refract Surg 2009; 25:1053–1060
18. He L, Sheehy K, Culbertson W. Femtosecond laser-assisted cataract surgery. Curr Opin Ophthalmol 2011; 22:43–52
19. Sanders DR, Higginbotham RW, Opatowsky IE, Confino J. Hyperopic shift in refraction associated with implantation of the single-piece Collamer intraocular lens. J Cataract Refract Surg 2006; 32:2110–2112
20. Norrby S. Sources of error in intraocular lens power calculation. J Cataract Refract Surg 2008; 34:368–376
21. Holladay JT. Refractive power calculations for intraocular lenses in the phakic eye. Am J Ophthalmol 1993; 116:63–66
22. Holladay JT. Standardizing constants for ultrasonic biometry, keratometry, and intraocular lens power calculations. J Cataract Refract Surg 1997; 23:1356–1370. Available at: http://www.docholladay.com/publications/StandardizingConstants.pdf. Accessed April 23, 2011
23. Wolffsohn JS, Buckhurst PJ. Objective analysis of toric intraocular lens rotation and centration. J Cataract Refract Surg 2010; 36:778–782
24. Walkow T, Anders N, Pham DT, Wollensak J. Causes of severe decentration and subluxation of intraocular lenses. Graefes Arch Clin Exp Ophthalmol 1998; 236:9–12
25. Nishimoto H, Shimizu K, Ishikawa H, Uozato H. New approach for treating vertical strabismus: decentered intraocular lenses. J Cataract Refract Surg 2007; 33:993–998
26. Morgan JE, Ellingham RB, Young RD, Trmal GJ. The mechanical properties of the human lens capsule following capsulorhexis or radiofrequency diathermy capsulotomy. Arch Ophthalmol

1996; 114:1110–1115. Available at: http://archopht.ama-assn.org/cgi/reprint/114/9/1110. Accessed April 23, 2011

27. Krag S, Thim K, Corydon L. Diathermic capsulotomy versus capsulorhexis: a biomechanical study. J Cataract Refract Surg 1997; 23:86–90
28. Singh D. Use of the Fugo blade in complicated cases [letter]. J Cataract Refract Surg 2002; 28:573–574
29. Kruger A, Amon M, Nepp J. Intraoperative and postoperative complications of high-frequency capsulotomy and continuous curvilinear capsulorhexis. J Cataract Refract Surg 1997; 23:429–432
30. Wilson ME Jr. Anterior lens capsule management in pediatric cataract surgery. Trans Am Ophthalmol Soc 2004; 102:391–422. Available at: http://www.pubmedcentral.nih.gov/picrender.fcgi?artid=1280111&blobtype=pdf. Accessed April 23, 2011
31. Izak AM, Werner L, Pandey SK, Apple DJ, Izak MGJ. Analysis of the capsule edge after Fugo plasma blade capsulotomy, continuous curvilinear capsulorhexis, and can-opener capsulotomy. J Cataract Refract Surg 2004; 30:2606–2611
32. Palanker D, Nomoto H, Huie P, Vankov A, Chang DF. Anterior capsulotomy with a pulsed-electron avalanche knife. J Cataract Refract Surg 2010; 36:127–132
33. Priglinger SG, Haritoglou C, Palanker D, Kook D, Grueterich M, Mueller A, Alge CS, Kampik A. Pulsed electron avalanche knife for capsulotomy in congenital and mature cataract. J Cataract Refract Surg 2006; 32:1085–1088
34. Priglinger SG, Palanker D, Alge CS, Kreutzer TC, Haritoglou C, Grueterich M, Kampik A. Pulsed electron avalanche knife: new technology for cataract surgery. Br J Ophthalmol 2007; 91:949–954. Available at: http://www.ncbi.nlm.nih.gov/pmc/articles/PMC1955651/pdf/949.pdf. Accessed April 23, 2011

OTHER CITED MATERIAL

A. Frey RW, Teuma EV, O'Suilleabhain D, Elliot D, Downes GR Jr, Downes GR III, Bielitzki J. Evaluation of the mechanical properties of the crystalline lens capsule following photodisruption capsulotomy and continuous curvilinear capsulorhexis. IOVS 2009; 50:. ARVO E-Abstract 1141. Available at: http://abstracts.iovs.org//cgi/content/abstract/50/5/1141?sid=7bea7e2d-94b3-4096-8135-901abfe2e6f4. Accessed April 22, 2011

First author:
Neil J. Friedman, MD

Mid-Peninsula Ophthalmology Medical Group, Palo Alto, California, USA